Supplement of Geosci. Model Dev., 19, 2111–2136, 2026
https://doi.org/10.5194/gmd-19-2111-2026-supplement

Geoscientific Model Development
Open Access
EGU

Supplement of

Development of the global chemistry-climate coupled model BCC-GEOS-Chem v2.0: improved atmospheric chemistry performance and new capability of chemistry-climate interactions

Ruize Sun et al.

Correspondence to: Lin Zhang (zhanglg@pku.edu.cn)

Table S1. Comparison of global annual emissions in BCC-GEOS-Chem v2.0

Main species	BCC-GEOS-Chem v2.0	BCC-GEOS-Chem v1.0	BCC-AGCM-Chem	Classic GEOS-Chem [a]
NO [b]	118.1	111.1	110.3	113.6
CO	926.2	925.5	1140.6	925.9
ISOP	389.4	410.0	410.8	367.2
Other species	**BCC-GEOS-Chem v2.0**	**BCC-GEOS-Chem v1.0**	**BCC-AGCM-Chem**	**Classic GEOS-Chem**
ALK4	54.7	44.0	\	52.9
BC	8.0	9.2	9.2	8.0
BENZ	7.8	6.7	\	7.8
C2H6	13.2	9.3	\	14.4
C3H8	14.5	7.2	\	14.4
CH2O	6.5	5.7	5.7	6.5
OC	29.5	31.0	31.0	29.5
PRPE	28.0	16.8	\	30.6
SO2	128.2	123.7	123.7	130.0
TOLU	8.5	7.8	\	8.5
XYLE	7.8	7.5	\	7.8

[a] Results from the standard version of GEOS-Chem v13.3.1 with aircraft emissions excluded (Wang et al., 2022). [b] Total NO emissions including lightning NO. All values are averaged over 2012-2014 in Tg yr^{-1}.

Table S2. Meteorological variables needed for GEOS-Chem v14.0.1.

NO.	Variables	Description	Usage	Unit
		2-D variables		
1	ALBD	Surface albedo	Dry deposition	1
2	CLDFRC	Cloud fraction	Photolysis	1
3	EFLUX	Latent heat flux	Diagnostics	W m^{-2}
4	FRSEAICE	Fraction of sea ice	Hg simulation	1
5	GWETROOT	Root soil wetness	Diagnostics	1
6	GWETTOP	Top soil moisture	CH_4 simulation	1
7	HFLUX	Sensible heat from turbulence	Dry deposition	W m^{-2}
8	FRLAND FROCEAN FRLAKE FRLANDIC FRSNO	Fraction of land/ocean/surface/snow/lake/land ice type in grid box	Chemistry	1
9	LAI	Leaf area index	Diagnostics	m^2 m^{-2}
10	PBLH	Planetary boundary layer height	PBL mixing	m
11	PRECCON	Convective precipitation	Wet deposition	mm day^{-1}

12	PRECTOT	Total precipitation	Wet deposition	mm day^{-1}
13	PARDR	Direct photosynthetically active radiation	Biogenic emissions	W m^{-2}
14	PARDF	Diffuse photosynthetically active radiation	Biogenic emissions	W m^{-2}
15	PHIS	Surface geopotential height	Diagnostics	m^2s^{-2}
16	TROPP	temperature based tropopause pressure	Grid setting	hPa
17	TS	Surface temperature	Chemistry,	K
	TSKIN	Surface skin temperature	deposition Sea salt emissions	K
18	TAUCLI	Optical depth of ice clouds	Diagnostics	1
19	TAUCLW	Optical depth of water clouds	Diagnostics	1
20	SUNCOS	Zenith angle	Chemistry	1
21	SNODP	Snow deposition	Diagnostics	m
22	SNOMAS	Snow mass	Dry deposition	kg m^{-2}
23	SWGDN	Surface incident radiation	Soil NOx; dry deposition	W m^{-2}
24	U10M	10m east-west wind speed	Dry deposition	m s^{-1}
25	USTAR	Friction velocity	Dry deposition	m s^{-1}
26	UVALBEDO	UV albedo	photochemistry	1
27	TO3	Total overhead O_3 column	Photolysis	DU
28	V10M	10m south-north wind speed	Dry deposition	m s^{-1}
29	Z0	Roughness length	Dry deposition	m
30	AREA_m^2	Grid box surface area	Many locations	m^2
31	XLAI	Leaf Area Index	Dry deposition	1
32	LANDTYPEFRAC	Olson fraction per land type	Dry deposition	1
		3-D variables on level edge		
33	PFILSAN	3-D flux of ice non-convective precipitation	Wet deposition	kg m^{-2} s^{-1}
34	PFICU	3d flux of ice convective precipitation	Wet deposition	kg m^{-2} s^{-1}
35	PFLLSAN	3-D flux of liquid non-convective precipitation	Wet deposition	kg m^{-2} s^{-1}
36	PFLCU	3d flux of liquid convective precipitation	Wet deposition	kg m^{-2} s^{-1}
37	CMFMC	Upward moist convective mass flux	Cloud convection	kg m^{-2} s^{-1}
38	PEDGE	Pressure edge for each grid	Grid setting	hPa
		3-D variables on level center		
39	CLDF	3-D cloud fraction	Chemistry	1
40	DTRAIN	Detrainment cloud mass flux	Cloud convection	kg m^{-2} s^{-1}
41	DQRLSAN	Large-scale rainwater source	Wet deposition	kg kg^{-1} s^{-1}
42	DQRCU	Convective rainwater source	Cloud convection	kg kg^{-1} s^{-1}
43	QI	Cloud ice water mixing ratio	Chemistry Aerosol microphysics	kg kg^{-1}

44	QL	Cloud liquid water mixing ratio - anvils	Chemistry Aerosol microphysics	kg kg^{-1}
45	RH	Relative humidity	Many locations	1
46	SPHU	Specific chemistry	Chemistry	kg kg^{-1}
47	T	Temperature	Chemistry	K
48	U	East-west component of wind	Advection	m s^{-1}
49	V	North-south component of wind	Advection	m s^{-1}
50	OMEGA	Updraft velocity	Diagnostics	Pa s^{-1}
51	REEVAPLS	Evaporation of precipitating LS & anvil condensate	Wet deposition	kg kg^{-1} s^{-1}
52	REEVAPN	Evaporation of precipitating convection condensate	Wet deposition	kg kg^{-1} s^{-1}
53	OPTD	Cloud optical depth	Photolysis	1

Table S3. Observations and reanalysis data used for model evaluation

Variables	Observation or reanalysis	Data sources or reference
Ozone	WOUDC network	http://woudc.org/data.php (last access: 1 Apr 2025)
	National monitoring networks	Wang et al. (2024)
	OMI satellite (Level 2)	Liu et al. (2010)
	Bodeker Scientific Filled Total Column Ozone	https://zenodo.org/records/7447757 (last access: 1 Apr 2025)
	MLS product (Level 3)	https://disc.gsfc.nasa.gov/datasets/ML3MBO3_005/summary?keywords=MLS%20O3 (last access: 1 Apr 2025)
NO_2	OMI satellite (Level 3)	https://disc.gsfc.nasa.gov/datasets/OMNO2d_003/summary (last access: 1 Apr 2025); Lamsal et al. (2021)
CH_2O	OMI satellite (Level 3)	https://h2co.aeronomie.be/ (last access: 1 Apr 2025); De Smedt et al. (2015)
CO	MOPITT satellite (Level 3)	https://terra.nasa.gov/data/mopitt-data (last access: 1 Apr 2025); Deeter et al. (2021)
$PM_{2.5}$	Satellite-derived $PM_{2.5}$	https://sites.wustl.edu/acag/datasets/surface-pm2-5/#TOOLS (last access: 1 Apr 2025); Shen et al. (2024)

SWDOWN OLR SWCRF LWCRF	CERES	https://ceres.larc.nasa.gov/data/ (last access: 1 Apr 2025); Kato et al. (2018)
Total precipitation	GPCP	https://psl.noaa.gov/data/gridded/data.gpcp.html (last access: 1 Apr 2025); Huffman et al. (2001)
TS Cloud fraction Cloud liquid water	MERRA-2	https://disc.gsfc.nasa.gov/datasets?keywords=MERRA-2&page=1 (last access: 1 Apr 2025)
T U-component wind V-component wind Omega	ERA5	https://cds.climate.copernicus.eu/datasets (last access: 1 Apr 2025)

Table S4. Time steps for each component in T42L26/T159L72 simulations.

Components	Time step (s)
Atmosphere (Chemistry/Emissions/Convection/Transport)	900/225
Land	900/225
Ocean	3600/900
Sea Ice	3600/900
Coupler	3600/900

Table S5. Reference pressures (Pa) under T42L26 and T159L72.

Level edge index	T42L26	T159L72
1	291.4067	0.7983
2	489.5209	1.8412
3	988.2418	3.8939
4	1805.2010	7.5847
5	2983.7240	13.6705
6	4462.3340	23.0105
7	6160.5870	36.4378
8	7851.2430	54.6051

9	9236.5800	77.8864
10	10866.3590	106.7850
11	12783.7080	141.3027
12	15039.3710	180.9154
13	17693.0430	225.1519
14	20814.9440	271.9188
15	24487.7090	320.4182
16	28808.5220	368.0077
17	33891.7310	414.4935
18	39871.8650	457.5551
19	46907.1800	505.4983
20	55183.8710	558.9235
21	64920.9690	618.5109
22	74438.2890	685.0316
23	83102.1230	759.3611
24	90330.0290	842.4946
25	95599.7460	935.4253
26	98511.2200	1038.9650
27	100000.0000	1154.3390
28		1282.9430
29		1426.3410
30		1586.2901
31		1764.7609
32		1963.9671
33		2186.3930
34		2434.8330
35		2712.4252
36		3022.6995
37		3369.6274
38		3757.6757
39		4191.8742
40		4677.8855

41		5222.0914
42		5831.3391
43		6511.8779
44		7271.8302
45		8120.4504
46		9068.0415
47		10126.0499
48		11307.0393
49		12625.0292
50		14095.5424
51		15735.8903
52		17565.4086
53		19605.6228
54		21880.8550
55		24403.9081
56		27157.7947
57		30156.2026
58		33415.3190
59		36952.5895
60		40785.8893
61		44934.0791
62		49416.9101
63		54254.6913
64		59469.0591
65		65082.1298
66		71117.2991
67		77598.9279
68		83529.3613
69		88748.7724
70		93113.8789
71		96503.1638
72		98821.1013

73		100000.0000

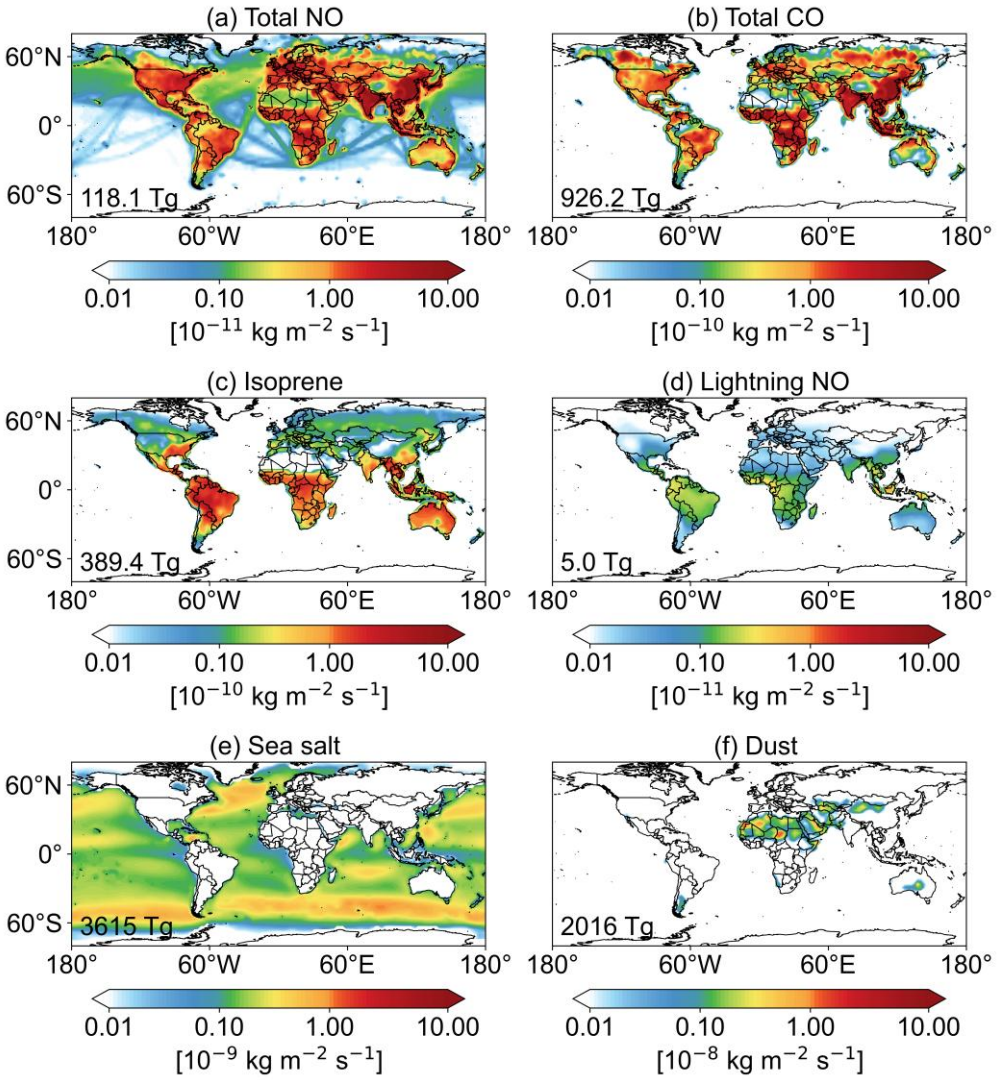

Figure S1. Spatial distributions of annual total emissions used in the study compared to Figure2 in Lu et al. (2020): (a) total NO emissions, (b) total CO emissions, (c) biogenic isoprene emissions, (d) lightning NO emissions, (e) sea salt emissions, and (f) mineral dust emissions. Values are averaged over 2012-2014.

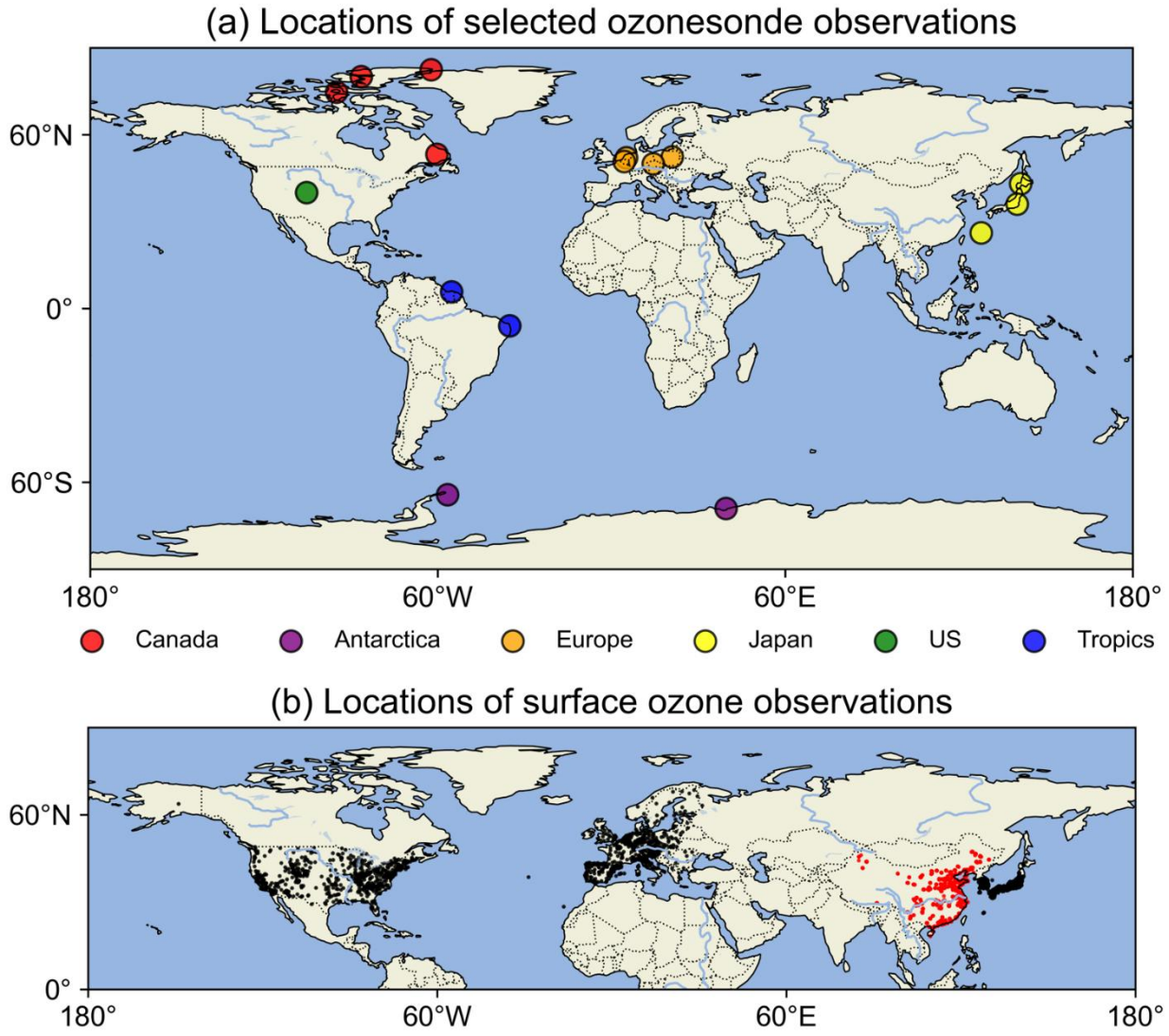

Figure S2. Locations of (a) selected ozonesonde observations, and (b) surface ozone observations used in this study. The black dots in panel b represent rural sites, which are used to evaluate surface ozone at T42L26 simulation, as we do not expect a coarse resolution simulation can resolve urban air pollution. The red dots represent observation sites in China used in Figure 10f. These sites are mostly located at urban or suburban regions.

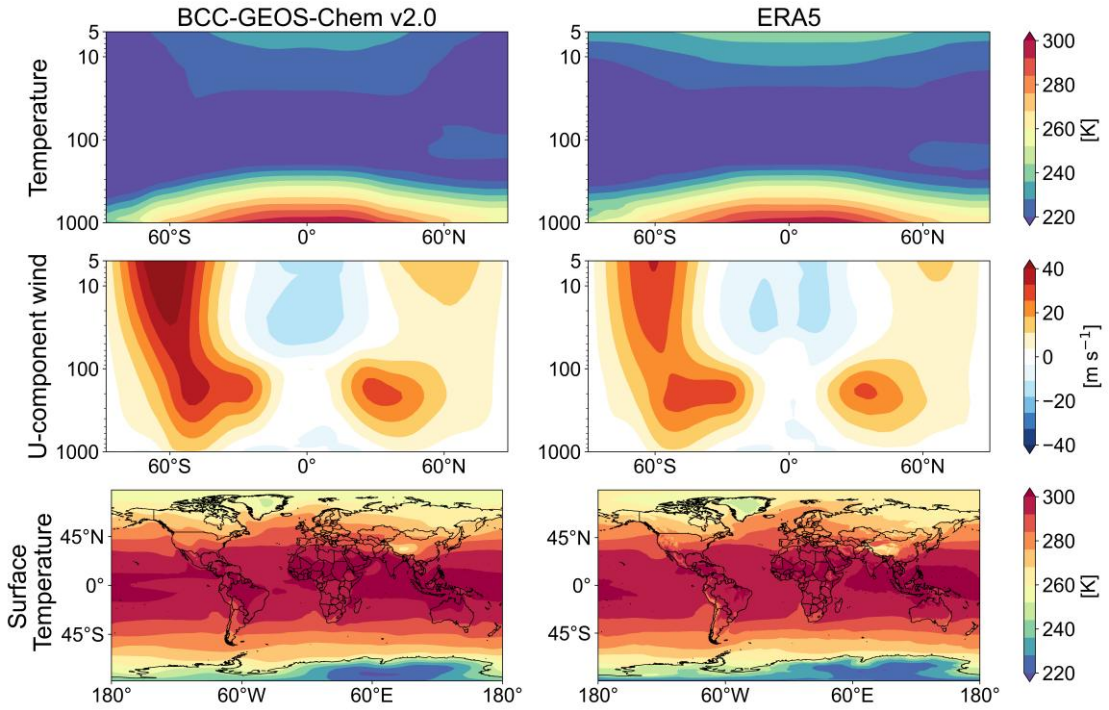

Figure S3. Zonal-mean temperature, U-component wind, surface temperature averaged over 2012-2014 from BCC-GEOS-Chem v2.0 under T42L26 configuration and ERA5 reanalysis.

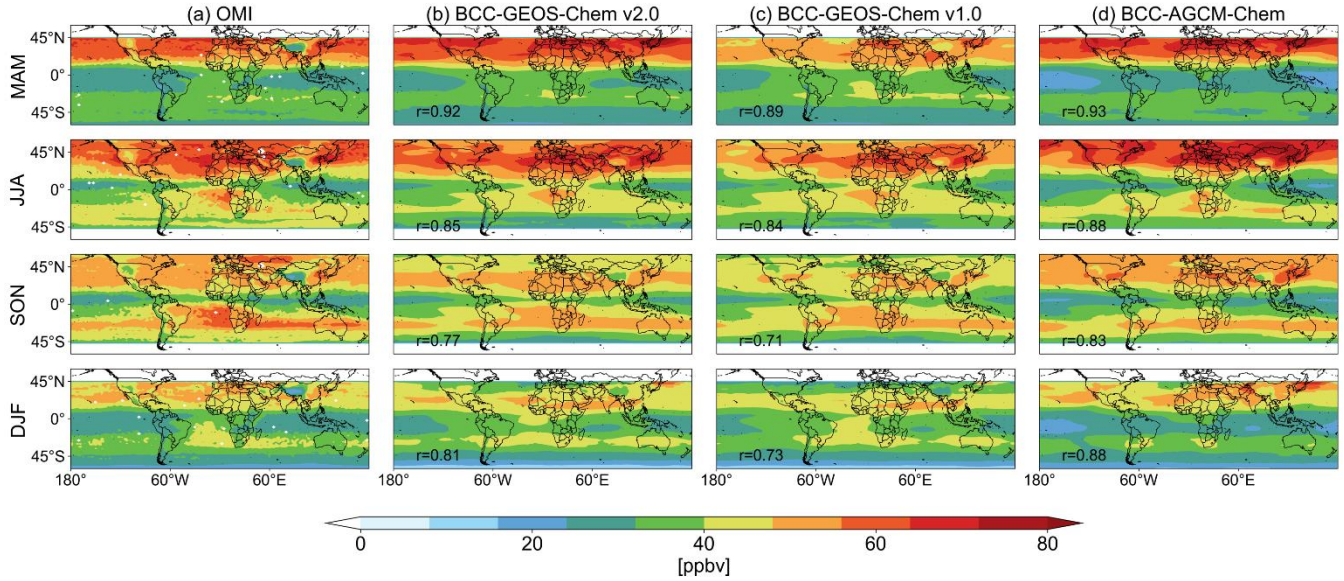

Figure S4. Spatial and seasonal distributions of global mid-tropospheric ozone averaged for 700-400hPa over 2012–2014 from (a) OMI satellite observation, (b) BCC-GEOS-Chem v2.0, (c) BCC-GEOS-Chem v1.0, and (d) BCC-AGCM-Chem. All model outputs are applied with OMI averaging kernels for a proper comparison with the observations.

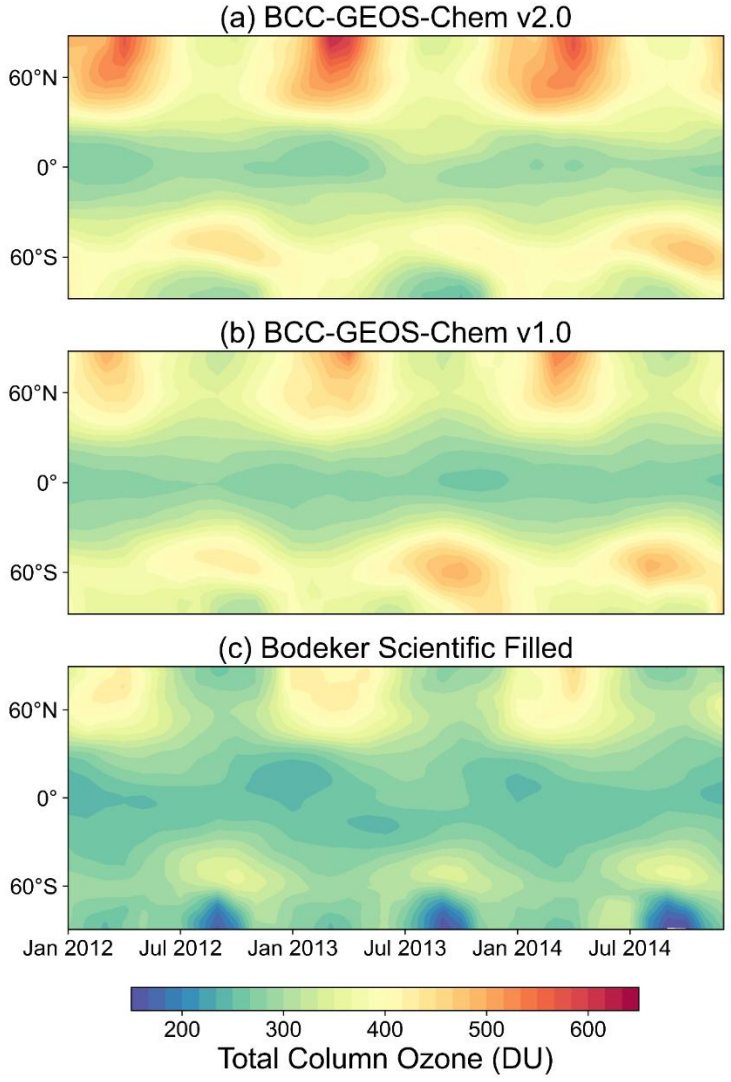

Figure S5. Zonal-mean column ozone over 2012-2014 from (a) BCC-GEOS-Chem v2.0, (b) BCC-GEOS-Chem v1.0, and (c) Bodeker Scientific Filled data.

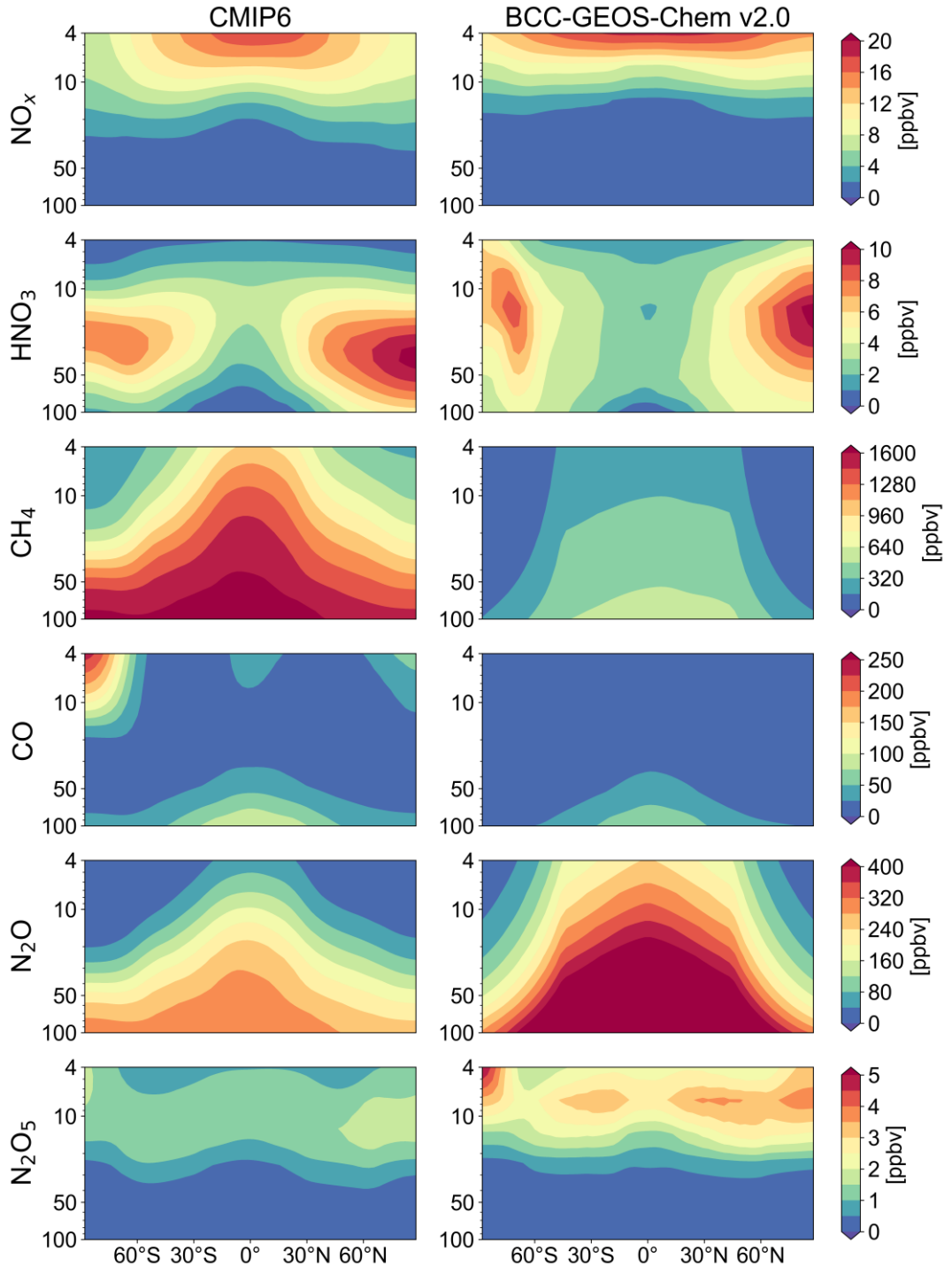

Figure S6. Zonal mean vertical distributions of NO_x, HNO_3, CH_4, CO, N_2O, N_2O_5 in the stratosphere from CMIP6 climatological field and BCC-GEOS-Chem v2.0 under T42L26 configuration.

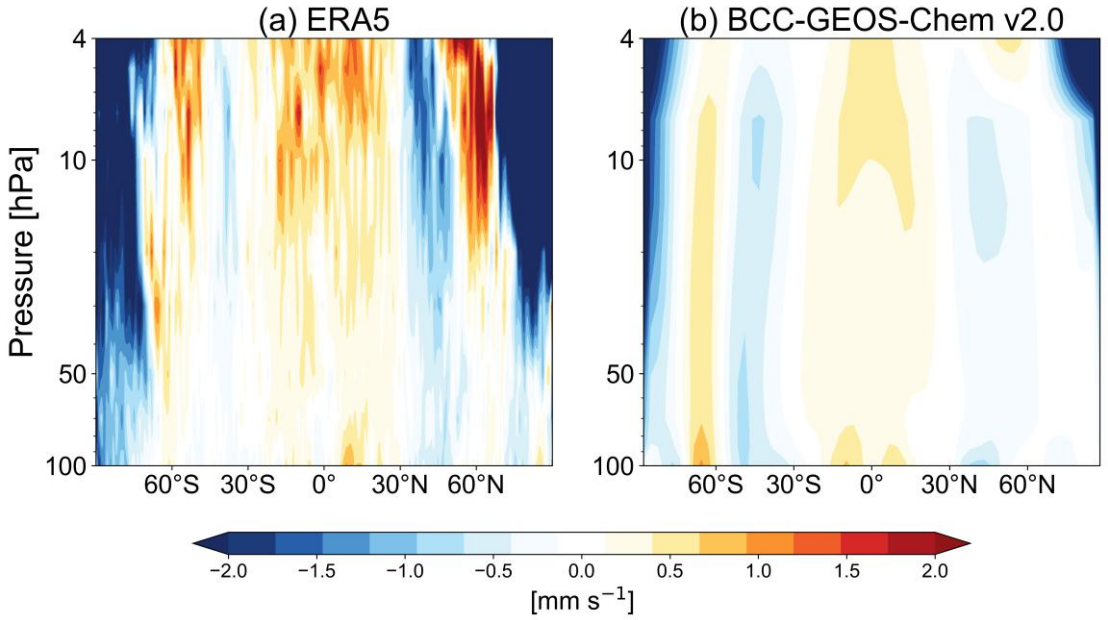

Figure S7. The vertical component of the residual circulation ($\overline{W}^*$) from (a) ERA5 reanalysis mean, and (b) BCC-GEOS-Chem v2.0 under T42L26 configuration. Values are averaged over 2012-2014.

60

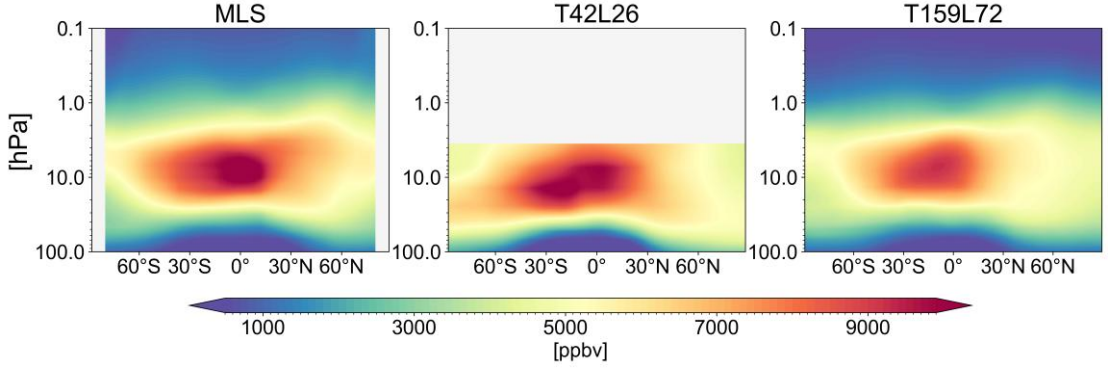

Figure S8. The zonal mean vertical distributions of ozone in the stratosphere from MLS and BCC-GEOS-Chem v2.0 under T42L26/T159L72 configuration. Values are averaged over January 2014.